Published in final edited form as:
J Nucl Med. 2009 May ; 50(5): 757–764. doi:10.2967/jnumed.108.058438.

Titration of Variant HSV1-tk Gene Expression to Determine the Sensitivity of ^{18}F-FHBG PET Imaging in a Prostate Tumor

Mai Johnson[1,2], **Breanne D.W. Karanikolas**[1], **Saul J. Priceman**[1], **Russell Powell**[1], **Margaret E. Black**[3], **Hsiao-Ming Wu**[1], **Johannes Czernin**[1], **Sung-Cheng Huang**[1], and **Lily Wu**[1,2]

[1]Department of Molecular and Medicalacology, UCLA, Los Angeles, California

[2]Department of Molecular, Cellular and Integrative Physiology, UCLA, Los Angeles, California

[3]Department of Pharmaceutical Sciences, Washington State University, Pullman, Washington

Abstract

Because of its high selectivity and specificity for the imaging reporter probe 9-(4-^{18}F-fluoro-3-[hydroxymethyl]butyl)guanine (^{18}F-FHBG), the herpes simplex virus type 1 thymidine kinase (HSV1-tk) variant sr39tk is actively being studied as a PET reporter gene. We recently demonstrated the capability of using a prostate-specific transcriptional amplification PET reporter vector, AdTSTA-sr39tk, to target prostate cancer lymph node metastasis. However, one area that warrants further study is the examination of the sensitivity of PET by determining the minimum percentage of cells expressing the sr39tk transgene needed for detection. Addressing this question could determine the sensitivity of vector-mediated sr39tk PET in cancer-targeting strategies.

Methods—DU-145, PC-3, and CWR22Rv.1 prostate cancer cell lines (a total of 1×10^6 cells) were studied, of which 7%, 10%, 25%, 50%, or 70% were transduced with the lentiviral vector constitutively expressing HSV1-sr39tk-IRES–enhanced green fluorescent protein (EGFP). Cells were subcutaneously implanted into the left shoulder of severe combined immunodeficient mice and evaluated. Tumor cells comparably transduced with an EGFP control vector were implanted on the right shoulder. Mice were imaged using PET with ^{18}F-FHBG at 8, 15, and 22 d after tumor implant. On day 23, tumors were isolated and analyzed for sr39tk transgene expression by quantitative reverse-transcriptase polymerase chain reaction (RT-PCR), Western blotting, immunohistochemistry, and flow cytometry for EGFP expression.

Results—Results showed a linear relationship between the level of sr39tk expression and the quantity of tracer accrual in DU-145, with the minimal value for PET detection at 10%. The magnitude of tracer retention in sr39tk-expressing cells was amplified over time as the tumor grew. Protein levels in the stepwise titration increased with the percentage of sr39tk-transduced cells.

Conclusion—The stepwise titration of prostate cancer cells transduced with the lenti-CMV-sr39tk-IRES-EGFP determined the minimum number of sr39tk-expressing tumor cells necessary to be detected by PET using the ^{18}F-FHBG reporter probe. Furthermore, PET signal correlated well with traditional methods of protein evaluation such as flow cytometry, quantitative RT-PCR, Western blotting, and immunohistochemistry. Unlike the traditional methods, however, the use of PET is noninvasive and will be more advantageous in clinical situations.

For correspondence or reprints contact: Lily Wu, Department of Molecular and Medical Pharmacology, UCLA, 675 Charles Young Dr. South, Los Angeles, CA 90095-1738. lwu@mednet.ucla.edu.

Keywords

prostate cancer; thymidine kinase; PET; transgene expression; lentivirus

According to the American Cancer Society, prostate cancer (PCa) remains the most commonly diagnosed cancer in U.S. men, with an estimated 186,320 new cases in 2008 (of which, 28,660 are projected to die of the disease) (1). Standard curative treatment options for patients with clinically localized cancer include radical prostatectomy, brachytherapy, and external beam radiation therapy. Anti-androgen therapies can be effective for the short term for patients who have metastatic or recurrent PCa, but most of these patients will eventually develop hormone-refractory disease that no longer responds to hormone treatments. The absence of effective therapies for hormone-refractory PCa establishes the need to develop novel therapeutic modalities for treatment and detection of advanced stages of the disease.

Molecular imaging techniques, such as PET to image transgene expression, offer great promise in clinical gene therapy trials. This noninvasive and highly sensitive approach can be used to monitor the biodistribution (2,3), magnitude (4,5), and persistence of the therapeutic gene expression over time (6,7). Viral vectors including the lentivirus and adenovirus are commonly used to deliver therapeutic and PET genes for cancer therapy studies (8–12). Herpes simplex virus type 1 thymidine kinase (HSV1-tk) has been well established as a suicide gene for the treatment of cancer and has been studied for more than 25 years (13,14). Thus, the ability to noninvasively monitor HSV1-tk transgene expression is highly desirable for both clinical and preclinical investigations.

The dual suicide and PET reporter functions of the HSV1-tk make it especially advantageous in an imageguided cancer therapy approach. As a suicide gene, the HSV1-tk encodes an enzyme that converts a nontoxic prodrug into a toxic metabolite, which can incorporate into DNA, causing chain termination and apoptosis (15). For more than a decade, HSV1-tk has been used as a reporter gene to image gene expression in living subjects (16). The mutant variant of the wild-type HSV1-tk gene, termed sr39tk, was developed to have enhanced binding affinity for the prodrug ganciclovir (17). In addition, sr39tk was later shown to increase PET sensitivity with the reporter probe 9-(4-^{18}F-fluoro-3-[hydroxymethyl]butyl)guanine (^{18}F-FHBG) (18–20).

Our group and others have successfully implemented ^{18}F-FHBG PET to monitor sr39tk suicide therapy in experimental PCa and glioma models on treatment with the prodrug ganciclovir (21–23). It would be valuable to further develop these promising sr39tk-based imaging and therapeutic approaches to target metastatic cancers. Recently, our group has demonstrated the capability of using a prostate-specific PET adenoviral vector, AdTSTA-sr39tk, to target PCa lymph node metastasis. ^{18}F-FHBG PET was able to detect lymph node metastasis due to vector-medicated sr39tk transgene expression, which was confirmed by immunohistochemical staining for HSV1-tk in the metastatic cancer cells (24). However, one area that warrants further investigation is the minimum number of sr39tk-expressing cells necessary to be detected by PET. Addressing this question could determine the sensitivity of vector-mediated sr39tk PET in cancer-targeting strategies.

In this study, we titrated the number of sr39tk-expressing cells in the PCa cell lines to determine the lower limit of cell number detectable by PET. We used lentiviral vectors to stably express sr39tk or enhanced green fluorescent protein (EGFP) under the control of the cytomegalovirus immediate early promoter (CMV) in these cell lines and established tumors with variable fractions of transduced cells for PET. The level of transgene expression in the tumor was analyzed by PET, quantitative reverse-transcriptase polymerase chain reaction (qRT-PCR),

Western blotting, immunohistochemistry, and flow cytometry. The ^{18}F-FHBG PET signals in the tumors significantly correlated with all of the gene expression assays.

MATERIALS AND METHODS

Lentiviral Production and Infection

The lentivirus was produced by triple transfections into 293T cells using the calcium phosphate transfection protocol (25). Virus-containing supernatants were collected at 48, 74, and 96 h after transfection, and the virus was quantified by detection of p24. The PCa cell lines DU-145 and PC-3 were maintained in Dulbecco's modified Eagle's medium, and CWR22Rv.1 was maintained in RPMI; all cell lines were supplemented with 10% fetal bovine serum and 1% penicillin and streptomycin and grown in a humidified incubator with 5% CO_2 and 95% air at 37°C. Lentiviral transductions in tissue culture were performed at a multiplicity of infection of 5. Cells were seeded at a density of 5×10^5 cells per well in a 6-well plate on day 0 then infected on day 1 in a maximum volume of 1 mL with 8 μg of Polybrene per milliliter (Sigma) for 6 h. On day 4, transduced cells were assayed for EGFP expression by flow analysis to determine transduction efficiency and counted for implantation in mice.

Flow Analysis for Tumor Implantation

Cells for flow analysis were prepared by trypsinization in 0.05% trypsin and 0.53 mM ethylenediaminetetraacetic acid (Mediatech). Samples were resuspended in 1× Dulbecco's phosphate-buffered saline (DPBS) and assayed on a flow cytometer (FACScan; BD Biosciences) at the UCLA Flow Cytometry Core. To make the different populations (50% tk, 25% tk, 10% tk, etc.) from the same initial population, the following equation was used: Desired % positive = ((no. of marked cells)(% EGFP positive))/ (no. of marked + no. unmarked), where unmarked cells are wild-type, untransduced cells.

Tumor Formation and Small-Animal PET/micro-CT

A total of 1×10^6 cells containing various percentages of sr39tk or EGFP control were implanted subcutaneously on the shoulder of male severe combined immunodeficient mice (Taconic Farms). PET for tk expression was performed by administering approximately 7,400 kBq (200 μCi) of ^{18}F-FHBG via the tail vein. After 1 h of tracer uptake, 10-min scans of the animals were obtained using a PET device (microPET Focus; Siemens Preclinical Solutions). Animals were then transferred to a micro-CT scanner (MicroCAT II; Siemens Preclinical Solutions). After attenuation correction (based on aligned CT image), all PET images were reconstructed by filtered backprojection. The spatial resolution of the reconstructed images was 1.75-mm full width at half maximum. To ensure accurate anatomic positioning, 3-dimensional ellipsoidal regions of interest (ROIs) were drawn on fused small-animal PET or micro-CT images. To minimize partial-volume effects, care was taken not to include the anatomic borders of the organs. Standardized uptake values (SUVs) for PET signals were obtained using a 2-mm ROI diameter, with quantification of decay-corrected regional activity normalized to injected dose concentration (i.e., injected dose divided by body weight) using the AMIDE software (26). Tumor volume was calculated on the basis of CT images. ROI sizes in micro-CT images were adjusted according to tumor size by placing the ROI around the tumor and adjusting the ROI depth to cover the entire tumor.

Flow Analysis at End of Study

To prepare single-cell suspensions of tumor samples, the tumor was minced into chunks with a scalpel and placed in serum-free RPMI medium. The medium and all remaining tumor chunks were collected and incubated for 20 min at room temperature with pronase at a final concentration of 10 mg/mL (Roche). Cells were washed with RPMI containing 10% fetal

bovine serum and allowed to recover overnight at 37°C with 5% CO_2 and humidity. On day 2, cells and remaining chunks were filtered through a 200-μm cell sieve to obtain single cells. The remaining tumor chunks from the sieve were collected and frozen for Western blot analysis. Single cells were subjected to a Ficoll extraction to remove cell debris. Briefly, cells were suspended in 5 mL of RPMI in a 15-mL conical tube and then underlayered with 2 mL of Ficoll-Paque PLUS (Amersham Biosciences). Any remaining space in the tube was filled with medium, and then the samples were spun at 1,500 rotations per minute with no brake for 15 min. Cell debris was pelleted at the bottom of the tube, and live cells remained at the Ficoll–medium interface. Live cells were collected, resuspended in 1× DPBS, and assayed by flow cytometry as described above.

Immunohistochemistry

A portion of the tumor was isolated and fixed in 10% buffered formalin (Fisher Scientific) overnight. Paraffin-embedded sections were cut 4 μm thick, baked for 1 h at 63°C, and deparaffinized and dehydrated by a series of xylene (10 min each × 3) and alcohol steps (100% for 2 min, 100% for 30 s, 95% for 30 s × 2, 70% for 30 s, 50% for 30 s; run under deionized water for 2 min). Antigens were retrieved by boiling the sections for 15 min in a citric acid and sodium citrate mixture (1:5). Slides were blocked in 0.3% hydrogen peroxide in methanol for 20 min, Power Block (Bio-Genex) for 10 min, and goat serum for 30 min. Slides were then incubated overnight with rabbit polyclonal anti-HSV1-tk antibody (provided by Dr. Margaret E. Black) at a 1:15,000 dilution. After rigorous washing, the slides were incubated with a 1:20 dilution of concentrated MultiLink (BioGenex) and washed rigorously a second time; concentrated HRP Label (1:20 dilution; BioGenex) was added, and then the slides were washed a third time. The slides were developed with DAB Peroxidase Substrate Solution (Bio-Genex) and counterstained with hematoxylin. To quantify sr39tk-positing cell content, tumor sections were photographed at 5 random fields (10× resolution), and positively stained cells were measured using software (ImageJ; National Institute of Health [NIH]). The average value of the fields from the NIH software was divided by the volume of the section (area multiplied by thickness) to obtain the number of positively stained cells per volume in cubic millimeters. This value was multiplied by the entire tumor volume as measured by CT to obtain the total cell number expressing the sr39tk gene.

Real-Time RT-PCR

Total cellular RNA was extracted from tumors using the RNeasy kit (Qiagen) according to the manufacturer's recommendation. RNA (0.5 μg) was reversed-transcribed using the iScript cDNA Synthesis Kit (BioRad) according to the manufacturer's recommendation. Real-time PCR was performed with 1 μL of cDNA per 25-μL reaction using the BioRad MyIQ Real-Time PCR Detection System with the following conditions: initial denaturation (95°C for 10 min), 40 cycles of denaturation (95°C for 30 s), annealing (60°C for 30 s), and elongation (72°C for 30 s). Sr39tk forward primer: 5′-AACATCTACACCACACAACACCGC-39, reverse primer: 5′-AAGGCATTGTTATCTGGGCGCTTG-3′. β-actin forward primer: 5′-TCAAGATCATTGCTCCTCCTGAGC-3′, reverse primer: 5′-TACTCCTGCTTGCTGATCCACATC-3′.

Western Blotting

Tumor chunks for Western blot samples were lysed in whole-cell lysis buffer (50 mM *N*-(2-hydroxyethyl)piperazine-N′-(2-ethanesulfonic acid), 150 mM sodium chloride, 1.5 mM magnesium chloride, 0.5 mM ethylenediaminetetraacetic acid, 10% glycerol, 1% Triton X-100 [VWR], 10 mM sodium fluoride, 1 mM dithiothreitol, and 1 mM phenylmethanesulfonyl fluoride, pH 7.0) by grinding with a pestle, followed by 3 freeze-and-thaw cycles and 30 min on ice. Samples were spun down at 4,000*g* for 5 min, and supernatants were transferred to

clean tubes; 20 μg of total protein per sample were separated by electrophoresis on 4%′20% Tris-HCl sodium dodecylsulfonate-polyacrylamide gel electrophoresis and transferred to nitrocellulose membrane overnight at 40 volts and 4°C. Membrane was blocked for 1 h at room temperature in 3% milk–phosphate–buffered saline-polysorbate. The following antibodies were used: anti-tk (Santa Cruz Biotechnology), anti-GFP (Invitrogen), anti-β actin (Sigma), horseradish peroxidase (HRP)–conjugated antigoat (Santa Cruz Biotechnology), HRP-conjugated antirabbit (Santa Cruz Biotechnology), and HRP-conjugated antimouse (Santa Cruz Biotechnology).

Statistical Analysis

SPSS software was used for statistical analysis (SPSS Inc.).

RESULTS

^{18}F-FHBG Uptake in DU-145, PC-3, and CWR22Rv.1 PCa Cell Lines

The growth characteristics and metabolic activity of PCa cell lines and tumors are heterogeneous. For instance, the functional activity of androgen receptors (AR), activity of receptor tyrosine kinases, or vascular growth factor levels can influence tumor growth kinetics and perfusion, which, in turn, could impact the uptake of metabolic tracers such as ^{18}F-FDG and fluorothymidine. Whether any of these perturbations could interfere with the uptake of ^{18}F-FHBG is unknown. Because the primary goal of this study was to quantify the number of cells expressing the sr39tk gene, it was important to select a cell line that provided specific ^{18}F-FHBG uptake. Therefore, 3 common PCa cell lines were examined. Two of the cell lines, DU-145 and PC-3, are androgen-insensitive and lack prostate-specific antigen (PSA) and AR. The CWR22Rv.1 PCa cell line expresses PSA messenger RNA and AR protein (27).

To assess sr39tk expression and ^{18}F-FHBG uptake, DU-145, PC-3, and CWR22Rv.1 cell lines were infected with lenti-cytomegalovirus-sr39tk-IRES-EGFP (multiplicity of infection, 5) to stably express sr39tk and EGFP reporter genes, under the control of a strong viral cytomegalovirus promoter. Lenti-cytomegalovirus-IRES-EGFP was used as the control vector. Cell populations were titrated by flow cytometry for EGFP to consist of either 7% stably transduced, GFP-positive cells plus 93% nontransduced cells (7%_sr39tk-IRES-EGFP or 7% _IRES-EGFP) or 70% stably transduced, GFP-positive cells plus 30% nontransduced cells (70%_sr39tk-IRES-EGFP or 70%_IRES-EGFP). A total of 1×10^6 tumor cells were implanted subcutaneously into the left (sr39tk) and right (EGFP control) shoulders of severe combined immunodeficient mice. Three weeks after implantation, mice were imaged with ^{18}F-FHBG. Figure 1A shows a differential uptake of ^{18}F-FHBG in these tumors. Robust accumulation of ^{18}F-FHBG was observed in tumors containing 70%_sr39tk-IRES-EGFP for DU-145 and PC-3 PCa cell lines but not in CWR22Rv.1 (left shoulder). No retention of ^{18}F-FHBG was seen in the DU-145 control tumor; however, some nonspecific accumulation of the tracer was observed in both PC-3 and CWR22Rv.1 control tumors (right shoulder). At the 7% sr39tk expression level, tracer uptake was not observed in the DU-145 tumor, and uptake in PC3 and CWR22Rv.1 was lower than that in the EGFP control. These results indicate that the PC-3 and CWR22Rv.1 cell lines exhibit discernable background accumulation of ^{18}F-FHBG, whereas retention in DU-145 is specific to the presence of the HSV1-sr39tk gene. We therefore selected the DU-145 PCa cell line to examine the relationship between sr39tk expression and ^{18}F-FHBG retention.

To achieve finer titration of the sr39tk expression, DU-145 tumors with 10%, 25%, or 50% EGFP-positive cells were established, with the sr39tk-expressing experimental tumors and EGFP-expressing control tumors implanted on the left and right shoulders, respectively. Eight

days after tumor cell implantation, specific accumulation of ^{18}F-FHBG from the sr39tk-expressing cells implanted on the left shoulder was detected in all 3 tumor groups (Fig. 1B). Moreover, the extent of sr39tk expression correlated with increasing ^{18}F-FHBG accumulation as calculated by SUVs. The magnitude of the tracer retention not only increased with rising sr39tk expression (TK50 > TK25 > TK10) but also amplified over time as the tumor volume increased (Fig. 1C). Hence, this stepwise titration provided a linear relationship between the level of sr39tk expression and quantity of tracer accrual.

Correlation of HSV1-sr39tk Transgene Expression by Molecular, Biochemical, and Histologic Assays

To measure the magnitude of HSV1-sr39tk expression in the tumors, conventional methods such as flow cytometry, Western blotting, quantitative RT-PCR, and immunohistochemistry were applied. Twenty-four hours after the last PET scan (day 23), animals were euthanized and several small portions of each tumor were analyzed using the methods mentioned above. As shown in Figure 2A, the percentage of EGFP-positive cells recovered from each tumor, as determined by flow analysis, displayed the same trend as the initially implanted populations. When tk messenger RNA expression was evaluated by quantitative RT-PCR, relative tk levels also increased with the increasing sr39tk-transduced population in the tumor (Fig. 2B). HSV1-sr39tk protein expression evaluated by Western blotting again exhibited an incremental increase among the 10%, 25%, and 50% groups (Fig. 2C). Finally, immunohistochemistry was performed to assess the extent of cells expressing the HSV1-sr39tk gene in the tumor. The degree of sr39tk-positive cell count in the tumor was estimated by image quantification. As shown in Figure 2D, HSV1-sr39tk staining increased with increasing transduction levels (from left to right). Finally, a cross-comparison of the expression profiles among the different methods such as PET, qRT-PCR, Western blotting, and immunohistochemistry showed a positive linear relationship, and the correlations between these relationships are statistically significant (Table 1; Figs. 3A–3D).

DISCUSSION

Systemic targeting and treatment of PCa metastasis using an adenovirus-based tk suicide gene system is actively being investigated (28–30). The capability to monitor tk gene expression in the targeted tissues would allow for a more complete assessment of gene transfer and therapeutic index. PET using the HSV1-tk gene and ^{18}F-FHBG reporter probe has been extensively established in both animal and human studies (31–33). The key objective of this study was to determine the cell number required for PET detection of sr39tk transgene expression using the ^{18}F-FHBG-reporter probe in a PCa model. Standard techniques such as flow cytometry, qRT-PCR, Western blotting, and immunohistochemistry were used to determine the gene expression level of the sr39tk PET reporter gene in DU-145 prostate tumors. As expected, the correlations among these standard molecular methods were statistically significant, confirming them as benchmark assays by which to measure sr39tk gene expression levels in tumors.^{18}F-FHBG PET signal (SUV) of the tumor was observed to correlate with all 4 standard molecular assays. These findings reaffirm the use of ^{18}F-FHBG PET as a noninvasive means for the measurement of HSV1-sr39tk gene expression in living subjects.

Among the 3 PCa tumor models examined (DU-145, PC-3, and CWR22Rv.1), DU-145 tumors displayed the most specific uptake of the ^{18}F-FHBG reporter probe with respect to sr39tk expression. The observed difference in uptake of ^{18}F-FHBG could be because of the varying degrees of vascularization among these tumors. However, in our experience, CWR22Rv.1 is the most highly vascularized tumor among the 3 models as determined by CD31-positive vessel density (data not shown). Differential substrate transport across the cell membrane or variable metabolic rates of the various cancer cell lines could also explain the difference in tracer uptake

(34). Therefore, the sensitivity and specificity of the ^{18}F-FHBG reporter probe for detecting sr39tk is cell type–dependent.

Given the specificity of the FHBG PET signal in the DU-145 tumor, an important issue to address is the overall sensitivity of the HSV-sr39tk-based reporter gene imaging. What is the minimal percentage of sr39tk reporter gene–transduced cells needed for detection using FHBG PET? Although it is difficult to determine the absolute number of sr39tk-positive cells in a tumor, this number can be estimated from our experiments. A PET signal was detectable in the TK10 group at 8 d after tumor cell implantation, in which 10% of 1×10^6 cells (i.e., 1×10^5 cells) were transduced (Fig. 1B). Conversely, when the number of sr39tk-positive cells was decreased to 70,000 in the 7% positive tumor, no specific PET signal was detected (Fig. 1A, DU-145). On the basis of these findings, a minimum of 100,000 tumor cells expressing sr39tk was needed to detect sr39tk gene expression by PET using ^{18}F-FHBG as a reporter probe. Although the cell number is based on the amount of cells initially implanted, at 8 d after implantation one might expect this number to be higher because of tumor growth. However, a significant lag in the formation of tumors in vivo, which generally take 1 wk to establish, was observed. Some cell death may initially take place until the tumor vasculature is established. Hence, it is not unreasonable to estimate the sr39tk-positive cell number to be 100,000 eight days after the initial implantation. This estimation is in line with an in vitro study performed by Fischer et al. in which they showed that the minimum number of cells required for a tumor to be detected by ^{18}F-FDG PET is 100,000 (35). Our results are also consistent with animal studies that used reporter PET in combination with optical imaging to quantify the number of T-cell trafficking in a collagen-induced arthritis mouse model (36,37).

The above determination of detection sensitivity is based on a tumor size of approximately 3 mm^3 (size at 8 d after implantation). For tumors of this size, the recovery coefficient due to partial-volume effect can be estimated from the results shown in Figure 1. We compared the data between 8 and 22 d in Figures 1B and 1C; the tumor volume increased from 3 to 180 mm^3 (with minimal partial-volume effect in the latter case), and the SUV increased by more than 3-fold. By assuming that the tumor cell density is constant over time, the recovery coefficient of tumors at day 8 is thus less than 0.3 (= 1/3). For larger tumors (with less partial-volume effect), the detection sensitivity is expected to be significantly higher.

Although we have determined the lower limit of PET detection in this study, it is premature to assume that this result will be directly applicable to other systems. Many factors could influence the sensitivity of reporter gene–based PET. Although the HSV-tk gene and its enhanced mutant sr39tk are the most extensively used, other PET reporter genes that have been developed include the dopamine receptor gene (38), sodium iodide symporter gene (39), and human somatostatin receptor (40). A thorough comparison of the in vivo imaging sensitivity for these PET reporter genes has not been accomplished.

In this study, we showed that the higher PET signal directly correlated with the proportion of sr39tk-positive cells within the tumor. It is also expected that the PET signal will correlate with the magnitude of reporter protein expressed per cell. In gene therapy studies, the strength of the gene regulatory promoter dictates the transgene expression level. We and others have developed several gene-amplification strategies to target PCa (41). The most effective strategy in our experience is to apply a 2-step transcriptional amplification (TSTA) method to modulate the prostate-specific but weak PSA promoter. The injection of an adenovirus that expresses the HSV-sr39tk gene under the TSTA system (AdTSTA-sr39tk) resulted in PET signals that exceed the strong constitutive viral cytomegalovirus promoter in prostate tumors (11,22,41). Importantly, the AdTSTA-sr39tk PET signal is produced in prostate tumor cells, which enables the specific and sensitive detection of nodal metastatic lesions of prostate tumors in mice (23). With the continual engineering of better PET reporter genes and reporter probes,

augmented expression strategies, and better instrumentations, investigators in molecular imaging can expect the sensitivity of reporter gene–based PET to continue to improve over time.

CONCLUSION

The capability of monitoring therapeutic gene expression in metastatic disease is important in the progress of cancer gene therapy. Here, PET was used to visualize the HSV1-tk-s39tk expression. The minimum number of sr39tk-expressing tumor cells necessary to be detected by PET using the ^{18}F-FHBG reporter probe was determined by performing a stepwise titration of PCa cells transduced with the lenti-cytomegalovirus-sr39tk-IRES-EGFP. The lower limit of detection was estimated to be 100,000 cells for tumors of size about 3 mm^3. HSV-sr39tk expression levels in these stepwise titrations were confirmed by conventional molecular techniques, such as flow cytometry, quantitative RT-PCR, Western blotting, and immunohistochemistry. The ^{18}F-FHBG PET signal was shown to correlate well with these 4 traditional methods.

Acknowledgments

This work could not be accomplished without the imaging technology infrastructure provided by the Department of Molecular and Medical Pharmacology and the UCLA Crump Institute for Biological Imaging in the School of Medicine at UCLA. We thank Dr. David Stout, Dr. Waldemar Ladno, and Judy Edwards for their skillful assistance with small-animal PET/micro-CT imaging. This work is in part supported by NIH/NCI R21 CA122693 and RO1 CA101904 and the UCLA Tumor Biology Program (USHHS Ruth L. Kirschstein Institutional National Research Service Award, T32 CA009056). Flow cytometry was performed in the UCLA Jonsson Comprehensive Cancer Center and Center for AIDS Research Flow Cytometry Core Facility, which is supported by NIH awards CA-16042 and AI-28697.

REFERENCES

1. American Cancer Society. Cancer Facts & Figures 2008. American Cancer Society; Atlanta, GA: 2008. Available at: http://www.cancer.org/downloads/STT/2008CAFFfinalsecured.pdf. Accessed March 17, 2009.
2. Nimmagadda S, Mangner TJ, Douglas KA, Muzik O, Shields AF. Biodistribution, PET, and radiation dosimetry estimates of HSV-tk gene expression imaging agent 1-(2′-deoxy-2′-^{18}F-fluoro-beta-D-arabinofuranosyl)-5-iodouracil in normal dogs. J Nucl Med 2007;48:655–660. [PubMed: 17401105]
3. Richard JC, Factor P, Welch LC, Schuster DP. Imaging the spatial distribution of transgene expression in the lungs with positron emission tomography. Gene Ther 2003;10:2074–2080. [PubMed: 14595380]
4. Hung SC, Deng WP, Yang WK, et al. Mesenchymal stem cell targeting of microscopic tumors and tumor stroma development monitored by noninvasive in vivo positron emission tomography imaging. Clin Cancer Res 2005;11:7749–7756. [PubMed: 16278396]
5. Xiong Z, Cheng Z, Zhang X, et al. Imaging chemically modified adenovirus for targeting tumors expressing integrin $\alpha_v\beta_3$ in living mice with mutant herpes simplex virus type 1 thymidine kinase PET reporter gene. J Nucl Med 2006;47:130–139. [PubMed: 16391197]
6. Dharmarajan S, Hayama M, Kozlowski J, et al. In vivo molecular imaging characterizes pulmonary gene expression during experimental lung transplantation. Am J Transplant 2005;5:1216–1225. [PubMed: 15888025]
7. Penuelas I, Mazzolini G, Boan JF, et al. Positron emission tomography imaging of adenoviral-mediated transgene expression in liver cancer patients. Gastroenterology 2005;128:1787–1795. [PubMed: 15940613]
8. Chang GY, Cao F, Krishnan M, et al. Positron emission tomography imaging of conditional gene activation in the heart. J Mol Cell Cardiol 2007;43:18–26. [PubMed: 17467733]
9. Freytag SO, Barton KN, Brown SL, et al. Replication-competent adenovirus-mediated suicide gene therapy with radiation in a preclinical model of pancreatic cancer. Mol Ther 2007;15:1600–1606. [PubMed: 17551507]

10. Sander WE, Metzger ME, Morizono K, et al. Noninvasive molecular imaging to detect transgene expression of lentiviral vector in nonhuman primates. J Nucl Med 2006;47:1212–1219. [PubMed: 16818958]
11. Sato M, Figueiredo ML, Burton JB, et al. Configurations of a two-tiered amplified gene expression system in adenoviral vectors designed to improve the specificity of in vivo prostate cancer imaging. Gene Ther 2008;15:583–593. [PubMed: 18305574]
12. Tarantal AF, Lee CC, Jimenez DF, Cherry SR. Fetal gene transfer using lentiviral vectors: in vivo detection of gene expression by microPET and optical imaging in fetal and infant monkeys. Hum Gene Ther 2006;17:1254–1261. [PubMed: 17134373]
13. Lal S, Lauer UM, Niethammer D, Beck JF, Schlegel PG. Suicide genes: past, present and future perspectives. Immunol Today 2000;21:48–54. [PubMed: 10637559]
14. Springer CJ, Niculescu-Duvaz I. Prodrug-activating systems in suicide gene therapy. J Clin Invest 2000;105:1161–1167. [PubMed: 10791987]
15. Culver KW, Ram Z, Wallbridge S, Ishii H, Oldfield EH, Blaese RM. In vivo gene transfer with retroviral vector-producer cells for treatment of experimental brain tumors. Science 1992;256:1550–1552. [PubMed: 1317968]
16. Tjuvajev JG, Stockhammer G, Desai R, et al. Imaging the expression of transfected genes in vivo. Cancer Res 1995;55:6126–6132. [PubMed: 8521403]
17. Black ME, Kokoris MS, Sabo P. Herpes simplex virus-1 thymidine kinase mutants created by semi-random sequence mutagenesis improve prodrug-mediated tumor cell killing. Cancer Res 2001;61:3022–3026. [PubMed: 11306482]
18. Alauddin MM, Conti PS. Synthesis and preliminary evaluation of 9-(4-[^{18}F]-fluoro-3-hydroxymethylbutyl)guanine ([^{18}F]FHBG): a new potential imaging agent for viral infection and gene therapy using PET. Nucl Med Biol 1998;25:175–180. [PubMed: 9620620]
19. Gambhir SS, Bauer E, Black ME, et al. A mutant herpes simplex virus type 1 thymidine kinase reporter gene shows improved sensitivity for imaging reporter gene expression with positron emission tomography. Proc Natl Acad Sci USA 2000;97:2785–2790. [PubMed: 10716999]
20. Min JJ, Iyer M, Gambhir SS. Comparison of [^{18}F]FHBG and [^{14}C]FIAU for imaging of HSV1-tk reporter gene expression: adenoviral infection vs stable transfection. Eur J Nucl Med Mol Imaging 2003;30:1547–1560. [PubMed: 14579096]
21. Jacobs AH, Rueger MA, Winkeler A, et al. Imaging-guided gene therapy of experimental gliomas. Cancer Res 2007;67:1706–1715. [PubMed: 17308112]
22. Johnson M, Sato M, Burton J, Gambhir SS, Carey M, Wu L. Micro-PET/CT monitoring of herpes thymidine kinase suicide gene therapy in a prostate cancer xenograft: the advantage of a cell-specific transcriptional targeting approach. Mol Imaging 2005;4:463–472. [PubMed: 16285908]
23. Yaghoubi SS, Barrio JR, Namavari M, et al. Imaging progress of herpes simplex virus type 1 thymidine kinase suicide gene therapy in living subjects with positron emission tomography. Cancer Gene Ther 2005;12:329–339. [PubMed: 15592447]
24. Burton JB, Johnson M, Sato M, et al. Adenovirus-mediated gene expression imaging to directly detect sentinel lymph node metastasis of prostate cancer. Nat Med 2008;14:882–888. [PubMed: 18622403]
25. Soneoka Y, Cannon PM, Ramsdale EE, et al. A transient three-plasmid expression system for the production of high titer retroviral vectors. Nucleic Acids Res 1995;23:628–633. [PubMed: 7899083]
26. Loening AM, Gambhir SS. AMIDE: a free software tool for multimodality medical image analysis. Mol Imaging 2003;2:131–137. [PubMed: 14649056]
27. Sobel RE, Sadar MD. Cell lines used in prostate cancer research: a compendium of old and new lines—part 1. J Urol 2005;173:342–359. [PubMed: 15643172]
28. Hsieh CL, Gardner TA, Miao L, Balian G, Chung LW. Cotargeting tumor and stroma in a novel chimeric tumor model involving the growth of both human prostate cancer and bone stromal cells. Cancer Gene Ther 2004;11:148–155. [PubMed: 14695756]
29. Nasu Y, Saika T, Ebara S, et al. Suicide gene therapy with adenoviral delivery of HSV-tK gene for patients with local recurrence of prostate cancer after hormonal therapy. Mol Ther 2007;15:834–840. [PubMed: 17327829]

30. Shirakawa T, Terao S, Hinata N, et al. Long-term outcome of phase I/II clinical trial of Ad-OC-TK/VAL gene therapy for hormone-refractory metastatic prostate cancer. Hum Gene Ther 2007;18:1225–1232. [PubMed: 18021019]

31. Miletic H, Fischer Y, Litwak S, et al. Bystander killing of malignant glioma by bone marrow-derived tumor-infiltrating progenitor cells expressing a suicide gene. Mol Ther 2007;15:1373–1381. [PubMed: 17457322]

32. Tjuvajev JG, Doubrovin M, Akhurst T, et al. Comparison of radiolabeled nucleoside probes (FIAU, FHBG, and FHPG) for PET imaging of HSV1-tk gene expression. J Nucl Med 2002;43:1072–1083. [PubMed: 12163634]

33. Yaghoubi SS, Couto MA, Chen CC, et al. Preclinical safety evaluation of ^{18}F-FHBG: a PET reporter probe for imaging herpes simplex virus type 1 thymidine kinase (HSV1-tk) or mutant HSV1-sr39tk's expression. J Nucl Med 2006;47:706–715. [PubMed: 16595506]

34. Germann C, Shields AF, Grierson JR, Morr I, Haberkorn U. 5-fluoro-1-(2′-deoxy-2′-fluoro-beta-D-ribofuranosyl) uracil trapping in Morris hepatoma cells expressing the herpes simplex virus thymidine kinase gene. J Nucl Med 1998;39:1418–1423. [PubMed: 9708520]

35. Fischer BM, Olsen MW, Ley CD, et al. How few cancer cells can be detected by positron emission tomography? A frequent question addressed by an in vitro study. Eur J Nucl Med Mol Imaging 2006;33:697–702. [PubMed: 16612588]

36. Su H, Forbes A, Gambhir SS, Braun J. Quantitation of cell number by a positron emission tomography reporter gene strategy. Mol Imaging Biol 2004;6:139–148. [PubMed: 15193248]

37. Yaghoubi SS, Creusot RJ, Ray P, Fathman CG, Gambhir SS. Multimodality imaging of T-cell hybridoma trafficking in collagen-induced arthritic mice: image-based estimation of the number of cells accumulating in mouse paws. J Biomed Opt 2007;12:064025. [PubMed: 18163841]

38. MacLaren DC, Gambhir SS, Satyamurthy N, et al. Repetitive, non-invasive imaging of the dopamine D_2 receptor as a reporter gene in living animals. Gene Ther 1999;6:785–791. [PubMed: 10505102]

39. Groot-Wassink T, Aboagye EO, Glaser M, Lemoine NR, Vassaux G. Adenovirus biodistribution and noninvasive imaging of gene expression in vivo by positron emission tomography using human sodium/iodide symporter as reporter gene. Hum Gene Ther 2002;13:1723–1735. [PubMed: 12396625]

40. Rogers BE, Parry JJ, Andrews R, Cordopatis P, Nock BA, Maina T. MicroPET imaging of gene transfer with a somatostatin receptor-based reporter gene and ^{94m}Tc-demotate 1. J Nucl Med 2005;46:1889–1897. [PubMed: 16269604]

41. Figueiredo ML, Sato M, Johnson M, Wu L. Specific targeting of gene therapy to prostate cancer using a two-step transcriptional amplification system. Future Oncol 2006;2:391–406. [PubMed: 16787119]

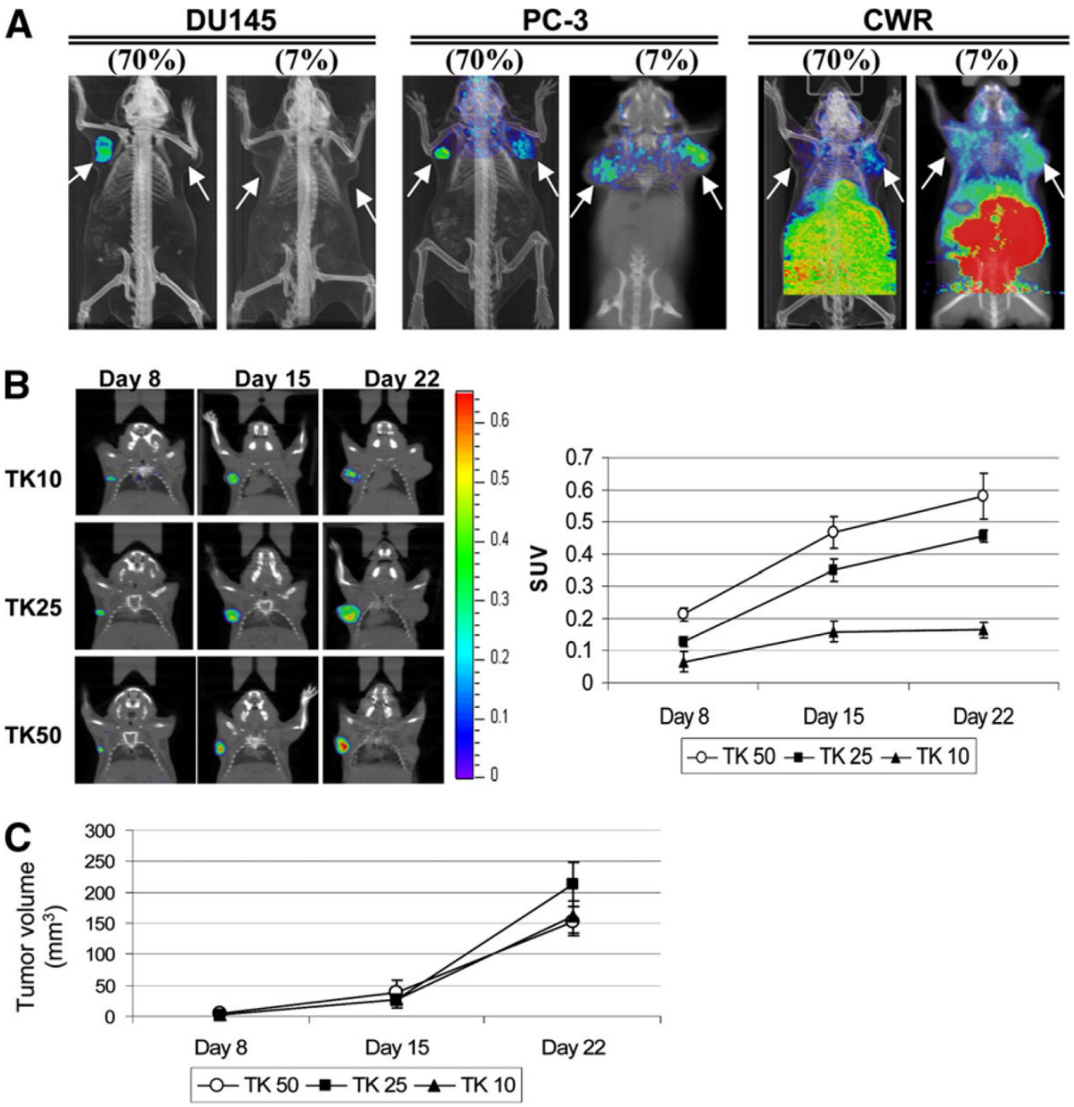

FIGURE 1.

Differential uptake of ^{18}FFHBG in DU-145, PC-3, and CWR22Rv.1 PCa cell lines. (A) Total of 7% or 70% of cells stably transduced with lentiviral vector expressing HSV1-sr39tk-IRES-EGFP or IRES-EGFP as control were implanted on left or right shoulder, respectively. Tracer uptake seen in abdominal area of all mice is indicative of clearance route but is cropped out in DU-145 and PC-3 for clarity. Arrows indicate tumor position. (B) DU-145 cells transduced with increasing levels of HSV1-sr39tk have higher ^{18}F-FHBG uptake (SUV), and intensity of signal increased over time with tumor volume (n = 4). (C) Tumor volume measure by CT was in range of 2.7–3.4 mm^3 on day 8, 26.9–38.1 mm^3 on day 15, and 152.8–212.8 mm^3 on day 22.

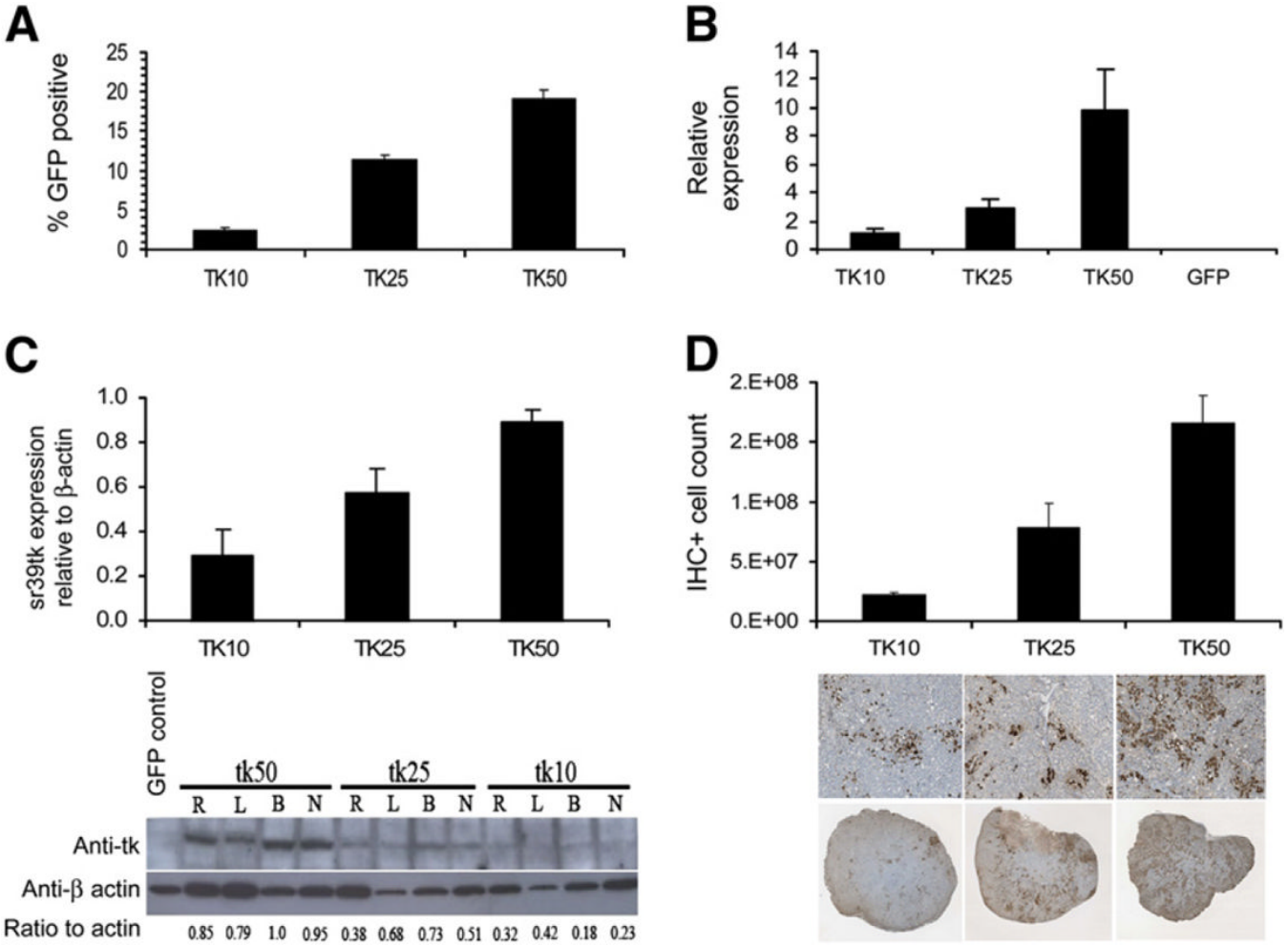

FIGURE 2.

HSV1-sr39tk transgene expression by flow, quantitative RTPCR, Western blotting, and immunohistochemistry. Tissues for these analyses were obtained from mice ($n = 4$) on day 23. (A) Single-cell suspensions of tumors were made, and percentage GFP-positive cells were obtained by flow analysis. (B) Quantitative RT-PCR analysis of sr39tk expression relative to β-actin levels. GFP tumor was used as a control. (C) Western blotting of sr39tk expression in tumor extracts. Sr39tk ratio to β-actin was analyzed using ImageJ (4 representative tumors per group shown). (D) Immunohistochemistry staining for tk protein in tumor sections. Number of cells positive for sr39tk expression increases with increasing percentage of lentiviral transduction. IHC+ = immunohistochemistry-positive; R, L, B, N = different animals within groups.

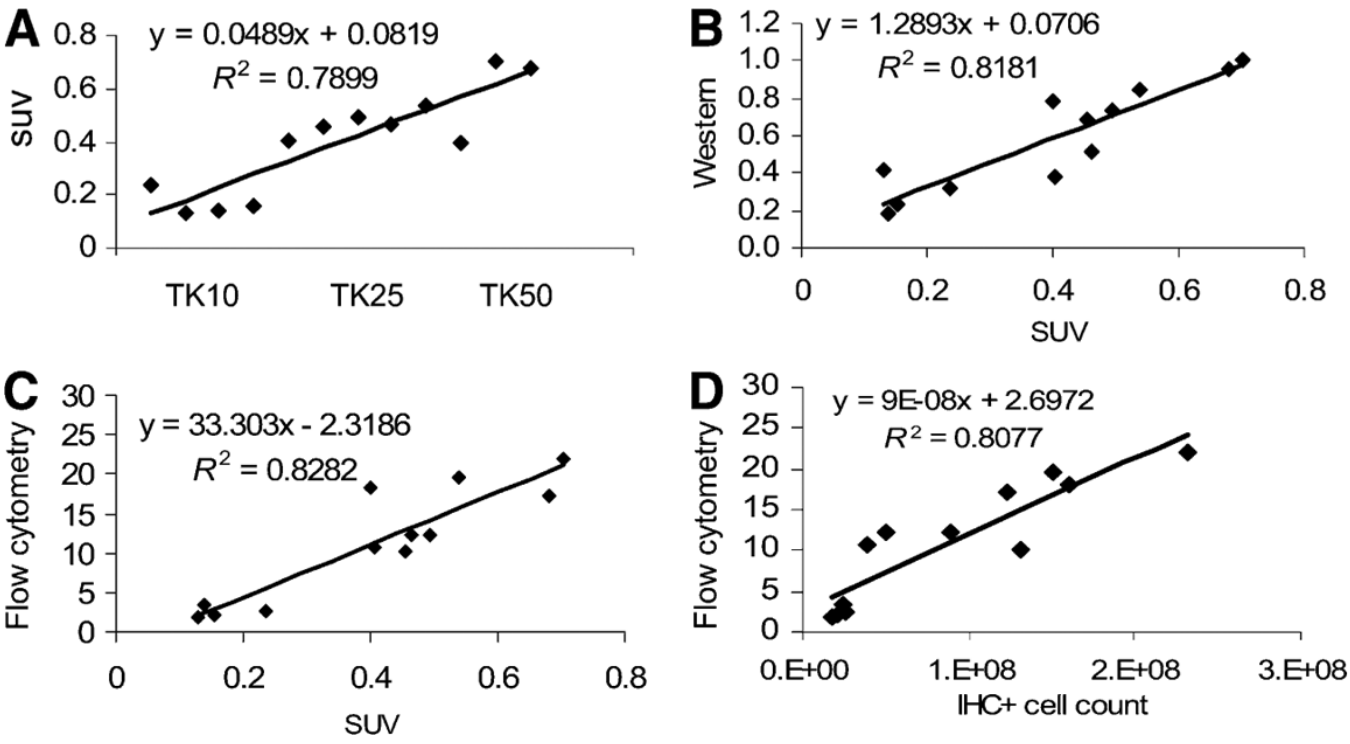

FIGURE 3.

Correlation of sr39tk expression among various methods (Table 1). (A) PET signal (SUV) and sr39tk-expressing groups. (B) Western blotting and PET signal. (C) Flow cytometry and PET signal. (D) Flow cytometry and IHC-positive cell count. IHC+ = immunohistochemistry-positive.

TABLE 1

Correlations of sr39tk Expression in DU-145 Cells Determined by Different Methods

		Method				
Method	**Parameter**	**SUV**	**Real-time RT-PCR**	**Cell no.**	**Western blotting**	**EGFP flow cytometry**
SUV	Pearson correlation	1	0.779*	0.803*	0.904*	0.911*
	Sig. (2-tailed)		0.003	0.002	0.000	0.000
	n	12	12	12	12	12
Real-time RT-PCR	Pearson correlation	0.779*	1	0.629†	0.740*	0.700†
	Sig. (2-tailed)	0.003		0.028	0.006	0.011
	n	12	12	12	12	12
Cell no.	Pearson correlation	0.803*	0.629†	1	0.869*	0.898*
	Sig. (2-tailed)	0.002	0.028		0.000	0.000
	n	12	12	12	12	12
Western blotting	Pearson correlation	0.904*	0.740*	0.869*	1	0.912*
	Sig. (2-tailed)	0.000	0.006	0.000		0.000
	n	12	12	12	12	12
EGFP flow cytometry	Pearson correlation	0.911*	0.700†	0.898*	0.912*	1
	Sig. (2-tailed)	0.000	0.011	0.000	0.000	
	n	12	12	12	12	12

Sig. = significant.

*Correlation is significant at the 0.01 level (2-tailed).

†Correlation is significant at the 0.05 level (2-tailed).

J Nucl Med. Author manuscript; available in PMC 2010 January 12.